Rödiger, T., Magri, F., **Geyer, S.**, **Mallast, U.**, Odeh, T., **Siebert, C.** (2020):
Calculating man-made depletion of a stressed multiple aquifer resource on a national scale
Sci. Total Environ. **725** , art. 138478

The publisher's version is available at:

http://dx.doi.org/10.1016/j.scitotenv.2020.138478

Calculating man-made depletion of a stressed multiple aquifer resource on a national scale.

Tino Rödiger[1], Fabien Magri[2,3], Stefan Geyer[4], Ulf Mallast[5], Taleb Odeh[6], Christian Siebert[4]*

[1] Helmholtz-Centre for Environmental Research UFZ, Dept. Computational Hydrosystems, Leipzig, Germany,

**email: tino.roediger@ufz.de*

[2] Freie Universität Berlin, Hydrogeologie, Berlin, Germany

[3] Bundesamt für die Sicherheit der nuklearen Entsorgung (Base), FA2, Berlin, Germany

[4] Helmholtz-Centre for Environmental Research UFZ, Dept. Catchment Hydrology, Halle, Germany

[5] Helmholtz-Centre for Environmental Research UFZ, Dept. Monitoring and Exploration Technologies, Leipzig, Germany

[6] Hashemite University, Zarqa, Jordan

Abstract: *An inexorable depletion of groundwater occurs where groundwater abstraction exceeds the natural recharge, a typical state of (semi-)arid regions, which calls for sustainable management of groundwater resources. This study aims to assess the available storage and recharge rates on a national scale in time and space by modelling the natural recharge in combination with a method to evaluate changing groundwater volumes, which revealed measures to quantify the overdraft of the observed national groundwater resources in Jordan. Applying the combination of hydrological model and method to evaluate changing groundwater volumes, a climate-driven systematic decline of groundwater recharge was eliminated as responsible process, while overdraft leads to dropping groundwater tables.*

The major findings are, the intensity of groundwater abstraction from a basin becomes visible through the fact, that simulated baseflow exceeds significantly the observed baseflow. About 75% of Jordan's groundwater basins are subject to intense groundwater depletion, reaching

annual rates of up to 1 meter in some basins. The most affected areas are the basins Zarka, Azraq and the predominantly fossil groundwater reservoirs in Southern Jordan.
Contrasting the past, when variable annual precipitation patterns did not negatively influence groundwater recharge, simulations show significantly reduced annual groundwater recharge all over Jordan. Particularly affected is the agricultural backbone in the Jordan Mountains, where recharge rates are predicted to vary between -30 mm/yr and +10 mm/yr in the coming decades, being reflected in the disappearance of freshwater springs and ascending saltwater.
The applied methodology is relevant and transferable to other data- and water scarce areas worldwide, allowing (i) a fast estimation of groundwater reservoir development on a national scale and (ii) an investigation of long-term effects of overdraft.

Key words: Hydrological modelling; Multi-response calibration; groundwater recharge; over-abstraction; depletion; climate change, semi-arid and arid regions, Jordan

1. Introduction

Particularly in regions, where aridity strongly limits the natural replenishment of exploitable water resources, water scarcity significantly restricts the environment and the socio-economic development (Alley et al., 1999; Dillon et al., 2012; UNCCD 2012; FAO, 2015). In addition, increasing population, expanding irrigated agricultural land and economic development results in a steadily growing demand for water, which can only be supplied by increasing abstraction of groundwater (Scheffran and Brauch, 2014; FAO, 2015). The consequences of overdraft are: i) dropping groundwater levels and associated dry-falling springs and production wells, and ii) intrusion and upconing of saltwater from the sea and deeper horizons, respectively. If an aquifer suffers from groundwater level dropping, called groundwater depletion (GWD), it is either the result of reduced groundwater recharge (GR), increased abstraction (V) or a combination of both. The problem of groundwater depletion is associated with deterioration in water quality due to the lack of a multi-year source of surface water, inadequate rainfall and excessive exploitation. That situation affects groundwater resources worldwide (Hanasaki et al., 2008; Gleeson et al., 2010; Purushotham et al., 2010; Litovsky et al., 2016; MacDonald et al., 2016; Houria et al., 2020). Groundwater depletion is even recognizable from space in more than 60% of the world's major aquifers (Richey et al., 2015). Nonetheless, a correct quantification of depletion is often missing due to sparse data (Rödiger et. al., 2014; Richey et al., 2015).

However, model-based aquifer management concepts must include groundwater depletion but often fail due to unavailability of abstractions rates, either due to missing metering or due to political issues. Since the early 1970s, when Jordan's industrialization significantly increased, population grew continuously but particularly from 2007 to 2020 from 6.1 to 10.2 Mio (World Bank 2020). The population increase caused tremendous groundwater overdraft and associated groundwater depletion. On national average the depletion reached values of 1 m/yr with highest rates of up to 2 m/yr in the basins along the western flank of the Jordan Highland (Goode et al., 2013).

Such depletion is either subject to climatic changes, which result in reduced groundwater recharge (GR) (Changnon, et al., 1988; Zektser & Loaiciga, 1993; Alley et al., 1999; De Vries & Simmers, 2002) or to overdraft (Gleeson et al., 2010). To evaluate both on the national scale is an objective of the present study. The evaluation is based on spatially discretized estimations of groundwater depletion for each of the 12 groundwater basins of Jordan for the last five decades. We analyzed the spatiotemporal variable natural water balance components applying the HBV-based hydrological model J2000g (Kralisch and Krause, 2006). Subsequently, the observed groundwater volume changes in the considered aquifers have been compared to the simulated groundwater recharge rates in order to estimate volumetric changes due to abstraction. Where available, estimated abstraction rates were compared to measured data to validate groundwater depletion. In a last step, representative concentration pathway (RCP) climate scenarios (RICCAR, 2020) were applied to force the calibrated hydrological model to predict changes in groundwater recharge for the region and to predict natural caused changes of groundwater tables in the next decades. By following a retrospective to forward-oriented perception on the development of groundwater resources on a national level, the present study is intended to provides an additional dimension to the analyses of such essential and hence strategic resource. Subsuming, this study aimed to find answers why available groundwater resources in the region show negative volumetric changes.

2. Study area

The Hashemite Kingdom of Jordan (ca. 89,400 km^2) is divided into three main physiographic provinces: i) the Jordan-Dead Sea-Rift Valley (JDSR), ii) the Western Mountain Highland and iii) the Eastern Desert, which covers ca. 70% of the territory (Fig. 1A). The meridional JDSR is a deeply incised valley that starts at mean sea level (msl.) at the Gulf of Aqaba, and drops to -430 m msl. at the Dead Sea and reaches -210 m msl. at Lake Tiberias (Fig. 1B). Parallel located to the JDSR is the Western Mountain Highland. With an average elevation of 900 m msl., it rises steeply from the JDSR and is frequently interrupted by deeply incised Wadis, which drain the highland. Eastward, the highland pass into the Eastern Desert Plain that reaches maximum altitudes of 900 m msl.

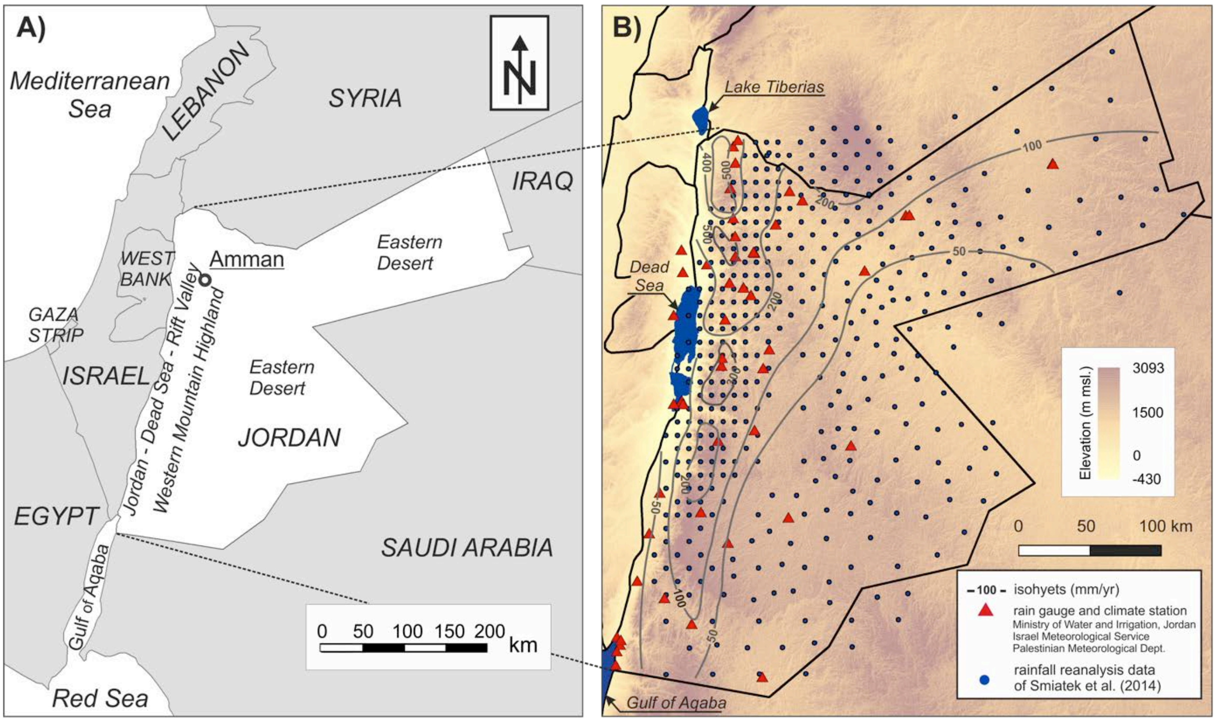

Fig. 1: A) *Location map of the study area and B) morphological overview showing isohyets, location of meteorological stations and the location of secondary data for rainfall analyses)*

The climate in Jordan is characterized by a strong gradient: Mediterranean with moderate rainfall of 200-600 mm/yr in the northwestern mountainous area to arid (<200 mm/yr) in about 90% of the country in the east and south (Fig. 1B). Precipitation is restricted to the hibernal months, while hot and dry climate prevails between April and September. Annual average temperatures are highest in the JDSR and in the Eastern Desert (30 °C) and lowest in the Western Highland (16°C).

Due to these dry climatic conditions, the only natural perennial surface water bodies of Jordan are the Dead Sea, which is shared with Palestine and Israel, the Lower Jordan River that emerges from Lake Tiberias and discharges into the Dead Sea and the Yarmouk River, which originates in the Syrian/Jordanian Hauran and feeds the Lower Jordan River (LJR). The Highlands are drained westward by ephemeral Wadis which either feed the LJR (Arab, Zarqa, Shueib, Kafrein and Hisban), or the Dead Sea (Mujib, Zarqa-Ma'aeen, Karak, Hasa and Ibn Hamad) (Fig. 2A).

The Ministry of Water and Irrigation divides Jordan's groundwater bodies into 15 basins (A-O in Fig. 2B), which depend on natural surface drainage basins and comprise a roughly 4,000m thick multi-layered aquifer complex. That aquifer package contains (i) the deep sandstone aquifer complex (DSA) of Paleozoic to Lower Cretaceous age, (ii) the upper aquifer complex (UCA) of Upper Cretaceous to Paleogene age and (iii) within the JDSR only a third, thin and shallow, locally used Cenozoic aquifer complex (CAC) exists (Fig. 2B).

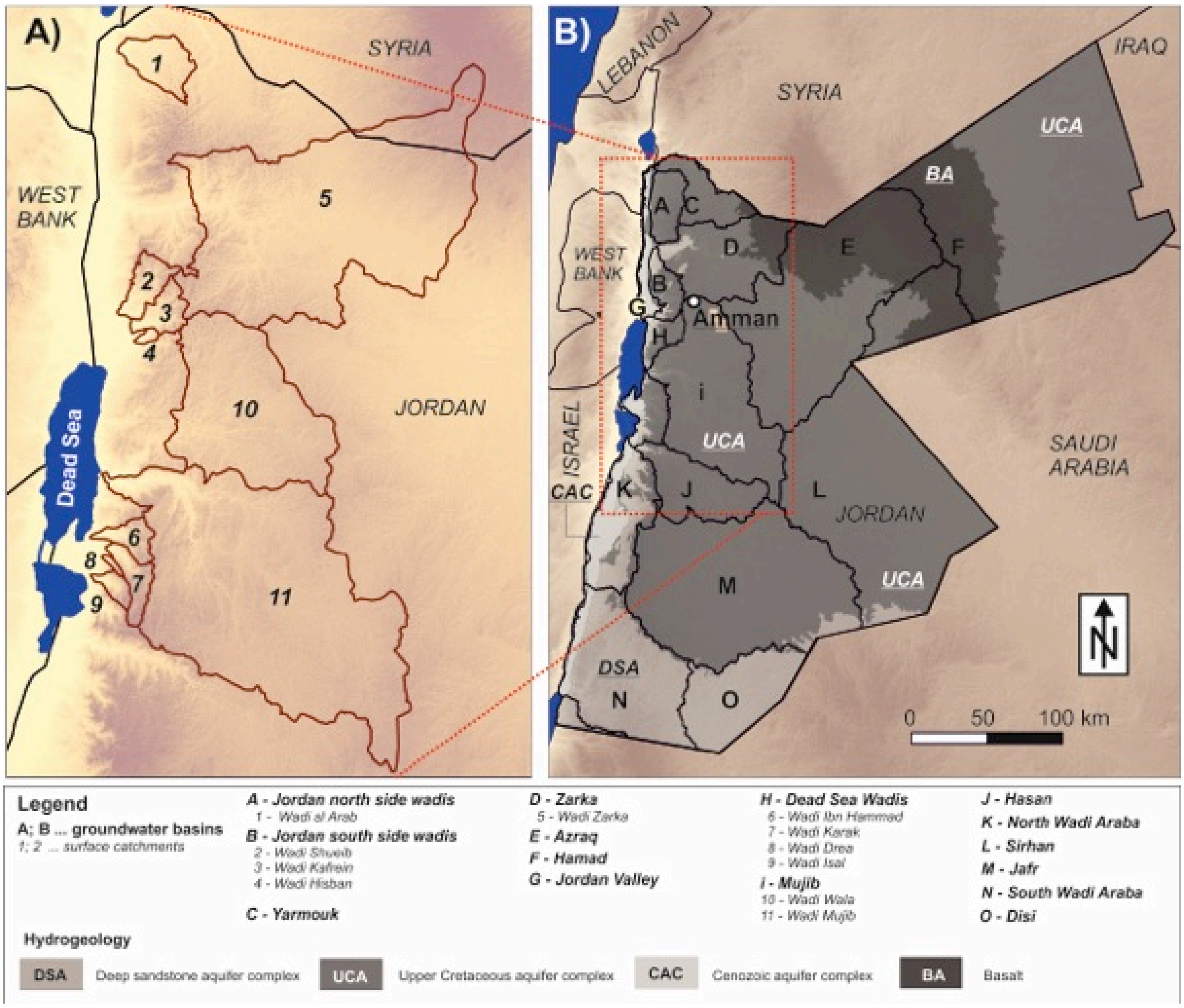

Fig. 2: *showing considered (A) surface and (B) groundwater basins in Jordan. Boundaries of the 15 groundwater basins (A-O) are taken from MWI (2015) and surface catchments (1-11) are calculated on the base of a 30m digital elevation model derived from the SRTM datasets, provided by USGS (2016). Only those basins are shown, which provide gauging information (MWI, 2015)*

Due to the fully arid conditions in the recharge areas of the DSA, groundwaters in that complex are considered to be non-renewable, contrasting the groundwaters hosted in the UCA and CAC. Following the dipping of the strata, groundwater in the DSA flows from its outcrops in the south northward and gets confined the moment the UCA overlies it. Contrastingly, groundwater in the UCA flows radial from the recharge area in the mountainous highland either northward towards the Yarmouk River, westward into the JDSR or eastward into the Azraq depression and the Eastern Desert.

3. Material and Methods

The hydrological model is based on 45-years long time-series (1970 - 2015) of monthly meteorological input data and in addition on spatially distributed information on topography, soil types and land-cover to describe the physio-geographical conditions of the study area. However, the setup of the model is challenging, since most watersheds in the region lack meteorological and hydrological measurements, and/or inconsistent or discontinuous time series or insufficient data quality. The spatial resolutions of alternative rainfall products (i.e. Tropical Rainfall Measuring Mission (TRMM) and Climate Prediction Centre Morphing Technique (CMORPH)) were too coarse to close the gap in meteorological data, since climatological gradients along the rift margins are extremely steep (Sachse et al., 2017). However, to generate a spatiotemporal consistent meteorological input dataset for the hydrological model missing rainfall data were complemented by re-analysis data (REA) (Smiatek et al., 2014). REA is based on rainfall data sets of the National Centres for Environmental Prediction (NCEP) and provide daily rainfall data with a spatial resolution of 6x6 km, fine enough to reproduce the intense climatic changes along the JDSR (Kunstmann et al., 2007). Furthermore, Representative Concentration Pathway (RCP), which is a greenhouse gas concentration (not emission) climate scenario adopted by the IPCC (IPCC, 2014) have been used to force the calibrated hydrological model to assess future possible changes in groundwater recharge over Jordan.

Climatological data. The applied climatological time series (MWI, 2015) comprise air temperature, radiation, wind speed and relative humidity from 55 stations and monthly precipitation data from 119 stations (Fig. 1B) collected between the years 1970 and 2015. The latter are predominantly distributed over the Western Highland, where the highest amount of rainfall occurs, while their density becomes extremely sparse elsewhere, particularly in the dry Eastern Dessert (Fig. 1B). In addition, 405 REA data sets were used, which simulate daily rainfall on an appropriate 6x6 km raster for the period 1970-2000 and allow hydrological modelling of the northern JDSR (Kunstmann et al., 2007). To assess the changes in groundwater recharge as a consequence of climatological changes, RCM-based predictions of precipitation changes (RICCAR, 2020) for two Representative Concentration Paths (i.e.

RCP 4.5 and RCP 8.5) were applied to force the calibrated hydrological model until the years 2046 and 2081, respectively. The results of all four simulation runs were translated into changes of groundwater recharge ∆GR according to Equation (1).

$$\Delta GR = GR_S - GR_o \qquad \text{(Eq. 1)}$$

with GR_S as average mean groundwater recharge of each of the four scenarios while GR_o is the mean groundwater for the time period 1970-2015. Negative numbers indicate a decline and positive numbers indicate an increase in GR.

Geographical information. Applying a 30x30 m SRTM DEM (USGS, 2016), slope and aspect were derived and the terrain was classified according to Tilch et al. (2002) into six slope ranges (*s*) (Table 1a), into eight 45°-wide aspect classes (*A*) (Table 1b), and their respective surface ratios.

Table 1a. *Classification of land surface into slope classes*

Slope range s	0°< - 2°	2°< - 5°	5°< - 10°	10°< - 15°	15°< - 20°	20°< - 30°
Surface ratio	0.41	0.47	0.07	0.03	0.01	0.01

Table 1b. *Classification of land surface into principal cardinal directions*

Cardinal direction	NNE	ENE	ESE	SSE	SSW	WSW	WNW	NNW
Surface ratio	0.42	0.08	0.08	0.17	0.11	0.06	0.08	0.003

Land cover was differentiated into 12 land cover classes analyzing ASTER images from May 2008. They were later reduced to five classes, which have been identified to be relevant for the model (Table 2). Specific parameterization variables like leaf area index and stomata resistance were adopted from literature (Dorman and Sellers, 1989; Körner, 1994; Schulze et al., 1994; Rödiger et al. 2014) and are given in Table 2.

Table 2: *Data for surface resistance and leaf area index of land covers used for the hydrological simulation (derived from Dorman and Sellers (1989); Körner (1994); Schulze et al. (1994); Rödiger et al. (2014).*

Land cover/ subclasses	Area (%)	Surface resistance of land cover (s/m)	Leaf Area Index (m^2/m^2)
Bare soil / sparse vegetation	84.73	120 – 150	0.2
Urban	0.59	20	-
Shrubs	9.32	102 – 323	0.8
Agriculture (cultivated)	3.82	141 – 303	0.17 - 0.53
Rangeland (grass)	1.54	80 – 1000	0.2 - 1.6

Soil properties (i.e. grain size, porosities, field capacities (*FCA*) and thickness) have been derived from National Soil Map of Jordan (Ministry of Agriculture, 1994) and used to discretize the land surface into 162 classes, which were subsequently aggregated within the respective morphological provinces (Table 3).

***Table 3**: Soil properties, derived from the National Soil Map of Jordan (Ministry of Agriculture, Jordan, 1994).*

Location	Order	Subclass	Area (%)	Depth (cm)	Field capacity (mm)
Jordan Valley	Ardisols	Ustochreptic and Ultisollic Camborthids	0.01	85 - 90	103 - 153
	Ardisols	Typic Calciorthids and Camborthids	0.05	67 - 90	102 - 128
	Entisols	Ustic Torriorthents and Torrifluvents	0.19	51 - 91	64 - 119
			total 0.24		
Western Highland	Ardisols	Typic and Lithic Camborthids	1.33	58 - 83	108 - 232
	Ardisols	Xerochreptic Camborthids and Calciorthids	6.20	35 - 90	53 - 178
	Ardisols	Typic and Lithic Calciorthids	1.23	48 - 92	73 - 133
	Entisols	Typic and Lithic Torriorthents	2.33	46 - 69	66 - 92
	Vertisols	Typic and Entic Chromoxererts	0.12	80 - 90	202 - 255
	Inceptisols	Calcixerollic, Lithic and Typic Xerochrepts	7.36	50 - 90	40 - 307
			total 18.57		
Southern Jordan	Entisols	Typic and Lithic Torriorthents	2.93	35 - 86	59 - 119
	Entisols	Typic and Lithic Torripsamments	3.31	62 - 85	94 - 194
	Ardisols	Typic Camborthids and Calciorthids	2.58	49 - 75	72 - 117
			total 8.81		
Central / Eastern Jordan	Ardisols	Typic Calciorthids and Camborhids	49.31	25 - 90	57 - 153
	Ardisols	Lithic Camborthids and Calciorthids	10.30	51 - 88	76 - 155
	Entisols	Typic, Xeric and Lithic Torriorthents	12.76	29 - 94	60 - 155
			total 72.37		

Discontinuous time series of groundwater level measurements were available for the period 1968-2006 and for 123 wells, distributed over the groundwater basins A-O (Fig. 2B) (MWI, 2015). Surface runoff data for the period 1970-2005 (MWI, 2015) were available for 13 surface catchments (Fig. 2A; Table 4). Among these catchments, Wadi Zarqa is outstanding since it perennially conveys on average 50 million cubic meters per year (MCM/yr) of treated wastewater (Al-Omari et al., 2009), which must be subtracted from the observed total discharge to receive natural flow patterns.

Table 4: *Shows characteristics of observed Wadis (catchment size; the percentage of DSA and UCA outcrops relative to the entire catchment, observed hydrological parameter and the time period of the data set.*

Name	Catchment (km^2)	Surface ratio of DSA* outcrop (%)	Surface ratio of UCA*** outcrop (%)	Time period	Observed data# (mm/d)
W. Wala	1803.0	0	100	01/81 - 02/98	total runoff
W. al Arab**	310	0	100	01/00 - 08/05	total runoff
W. Mujib	4448.6	1	99	10/84 - 09/99	baseflow
W. Zarka	4318.5	12	88	10/69 - 10/05	total runoff
W. Karak	155.9	12	88	01/81 - 09/02	total runoff
W. Ibn Hamad	128.1	16	84	01/81 - 09/99	baseflow
W. Shueib	179.2	16	84	09/81 - 08/99	baseflow
W. Hisban	77.0	28	72	10/82 - 09/99	baseflow
W. Isal	68.7	36	64	10/78 - 05/97	baseflow
W. Kafrein	158.8	40	60	10/85 - 09/99	baseflow
W. Drea	26.2	45	55	12/80 - 09/99	baseflow

** subsurface area *Deep Sandstone Aquifer ***Upper Cretaceous Aquifer # source: MWI (2015)

Data for mean storage coefficients *S* (Table 5) were derived from literature (El-Naqa, 1993; Ayed, 1996; Abdullah et al., 2000, Abdullah and Al-Assa'd, 2006; Rimawi et al., 2012; UN-ESCWA and BGR, 2013; Shawaqfah et al., 2016). The maximum percolation capacities of each geological unit (Fig. 2B) were derived from Berndtsson and Larson (1987).

Table 5: *Characteristics of groundwater basins.*

Basin	Name of gw basin	Total catchment area A_T (km^2)	Aquifer outcrop area A_O (km^2)	GR_A mean gw recharge (MCM/yr)	Total aquifer area A_A (km^2)	Mean water level change Δh (m)	Observation period Δh (year)	Storage coefficient S	Total gw abstraction (MCM)	V_A mean annual abstraction (MCM/yr)	Knwon abstraction (MCM/yr)	GWD groundwater depletion (MCM/yr)
A	North rift side Wadis	26.8		2.3	26.8	5.09	1985 - 2006	0.03	4.23	0.20	-	2.08
A - 1	W. al Arab	320		18.3	320	71.98	1982 - 2006	0.02[B]	460.67	19.19	20.8[A]	-0.89
B	South rift side Wadis	684		32.78	684	4.79	-	-	-	-	-	-
C	Yarmouk	1458		31.2	1458	33.43	1974 - 2006	0.02	975.31	37.51	62.8[A]	-6.35
D	Zarka (total)*	4318	-	95.0	-	-	-	-	-	-	-	-
	***productive aquifer A7/B2**		1748	56.3	3725	27.55	1968 - 2006	0.03[G]	3078.71	118.41	83.4[A]	-62.14
E	Azraq (total)	11669		26.89	-	-	-	-	-	-	51.4[A]	-
	productive aquifer B4/B5	-	6919	14.4	6919	9.48	1985 - 2006	0.015[F]	984.26	46.87	43.1[A]	-32.46
	aquifer basalt	-	4749	-	4749	11.85	1986 - 2006	0.003[F]	168.82	8.44	-	-
F	Hamad (total)*	14436	-	23.5		-	-	-	-	-	-	-
	***productive aquifer B4/B5**	-	9921	11.9	9921	0.55	1971 - 2006	0.015	81.85	3.15	1.9[A]	8.72
G	Jordan Valley	706		13.95	706	9.96	1980 - 2006	0.02	140.64	5.41	17.0[A]	8.54
H + i + J	Surface Dead Sea basin	10448	-	174.1	-	-	-	-	-	116.79	79.4[A]	-
H	Dead Sea side Wadis	1423	-	50.9	-	-	-	-	-	-	-	-
i - 12	Wala (total)*	1803	-	41.4	-	-	-	0.015[C]	-	-	-	-
	***productive aquifer A7/B2**	-	778	24.9	1803	32.64	1985 - 2006	0.015[C]	882.75	42.04	-	-17.13
i - 13	Mujib (total)*	4449	-	52.0	-	-		0.015[C]	-	-	-	-
	***productive aquifer A7/B2**	-	2514	40.7	4440	20.12	1985 - 2006	0.010[C]	1339.99	63.81	-	-23.06
J	Hasan (total)*	2773	-	29.9	-	-	-	-	-	-	-	-
	***productive aquifer A7/B2**	-	1253	15.9	2595	10.85	1988 - 2006	0.007	197.09	10.95	-	4.95
K	North Wadi Araba	2939	-	34.41	2939	2.51	1979 - 2006	0.02	147.54	5.67	6.3[A]	28.74
L	Sirhan	16383	-	15.9	16383	-	-	-	-	-	-	-
M	Jafr	12542	-	27.34	12542	9.68	1988 - 2006	0.006[E]	728.44	40.47	35[A]	-13.13
N	South Wadi Araba	5996	-	22.8	5996	1.05	1975 - 2006	0.02	125.92	4.84	8.5[A]	14.28
O	Disi	5734	-	11.2	5734	12.87	1982 - 2006	0.02[D]	1475.93	61.50	90[D]	-50.32
	Jordan (study area)	89400		529.6	-	-	-	-	-	-	-	-
	Subsurface Dead Sea basin	66951		483.3	-	-	-	-	-	-	-	-

Data source: [A] MWI Jordan; [B] Roediger et al. (2014); [C] El-Naqa (1993); [D] UN-ESCWA and BGR (2013); [E] Rimawi et al. (2012); [F] Ayed (1996); [G] Shawaqfah et al. (1999)

To evaluate the mid- to long-term changes of groundwater volumes, above described data and methodologies have been used following the flowchart in Figure (3), which is described in detail in the following chapters.

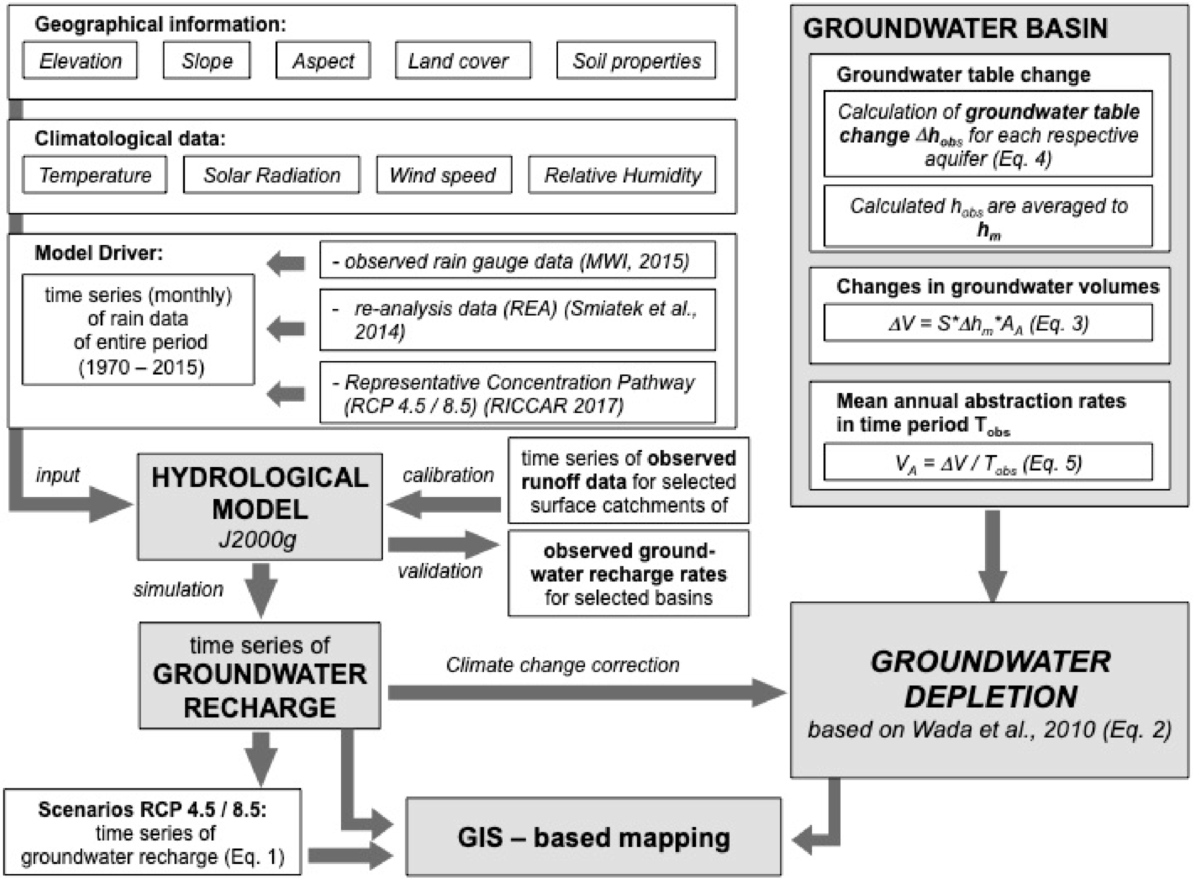

Fig. 3: *Flowchart of methods used in this study.*

4. Modelling Runoff and Groundwater Recharge

4.1 Model Setup

Natural groundwater recharge and runoff were estimated for all 15 groundwater basins of Jordan (Fig. 2B; Table 5) applying the hydrological model J2000g. The core of J2000g is the soil moisture balance module, which calculates the hydrological water balance components (evapotranspiration (*ET*), groundwater recharge (*GR),* direct runoff (*DQ*) and soil moisture content) by taking spatially distributed information about topography, land use, soil type and climatological input data (rainfall, air temperature, sunshine duration, relative air humidity, wind speed) (Fig. 3). The detailed mode of operation of J2000g is given in Krause (2001), Krause and Hanisch (2009) and Krause et al. (2010).

To spatially discretize the study area, a mesh of regular square elements with varying edge lengths (500m, 1,000m and 2,000m) was generated. The element size was defined according to the morphological, climatological and resulting hydrological gradients in a way that the mesh became finer the stronger gradients are. Hence, within the Western Mountain Highland with steep hydrological gradients and sufficient density of climate data, elements of 500 m edge length were defined, while the plains in the east and southeast, with low morphological and climatological gradients are represented by a mesh with edge lengths of 1-2 km. The basic mesh was intersected with the river network, whereby additional irregular polygonal elements were generated. All input parameters were spatially integrated to generate a spatially discriminated mesh of 88,398 so called hydrological response units (HRU). An HRU is assumed to respond hydrologically homogenous (Flügel, 1993).

To calculate water balance components for each HRU, discrete climatological input data have to be spatially interpolated by inverse distance weighting and optional elevation correction. Accounting for the coarse temporal resolution of the climatological input data, the calculation is pursued in monthly time steps. For each time step, the model allocates the soil water content for each HRU considering the soil type specific maximum field capacity (*mFC*). Soil moisture storage below *mFC* can be emptied by *ET* only. Potential evapotranspiration (*PET*) is calculated using Penman–Monteith (described in e.g. Allen et al. (1998)) and can be adjusted globally for all HRUs by a calibration parameter β (Table 6).

Runoff from HRUs is produced, when rainfall intensity exceeds the infiltration capacity of the soil or soil moisture exceeds *mFC*. Then, runoff is divided into *GR* and *DQ*. The ratio between both is controlled by surface slope (α) and the ratio of vertical to horizontal discharge (*LVD*), which varies between 0 and 1. The generated *GR* is further split by the calibration coefficient (γ) into two groundwater reservoirs, which react fast (GWS1) and slow (GWS2). Each of the reservoir types is characterized by a retention coefficient (*k*) and represented by a linear storage cascade (Nash, 1958) of *n* reservoirs and forms baseflow (*BQ*). Eventually, total stream flow of a catchment is the sum of *DQ* and *BQ* from each HRU.

Most of the observed catchment areas are dominated by outcropping UCA (Table 4). Hence, an initial uncalibrated J2000g model was set up with an a-priori parameter set (Table 6), which has been successfully applied in a typical UCA catchment with a double porosity aquifer (Wadi Al Arab, cf. Rödiger et al. (2014)).

Table 6: *A-priori input parameter for the initial uncalibrated model run*

Parameter	Value	Implication
mFC	1	National Soil Map of Jordan*; (*Ministry of Agriculture, Jordan, 1994)
β	1.2	Correction factor for the calculated PET (1.2 slight increasing PET)
LVD	0.7	increased vertical discharge
γ	0.7	70% fast (DSW1) and 30% slow (DSW2)
k_1	1.75	well-drained karst aquifer
n_1	4	
k_2	45	considerable matrix flow of the aquifer
n_2	2	

4.2 Parameterization

To determine the ability of the model to reproduce measured total surface runoff as a function of the applied rainfall input datasets, in particular the usability of REA, three runs were performed as initial test to compare simulated versus observed runoff data applying i) available rain gauge data, ii) REA data and iii) a combination of rain gauge and REA data. Correlation coefficients of determination were calculated for each catchment and finally combined to a mean R^2 value. The results indicate that for runs driven by rain gauge data, the simulated runoff exceeds the observed runoff, while results are inverted for REA driven simulations. Figure 4 shows results for two exemplary catchments. Since the best results are achieved when taking a combined input file, containing rain gauge and REA data, the model's calibration was performed using these combined datasets.

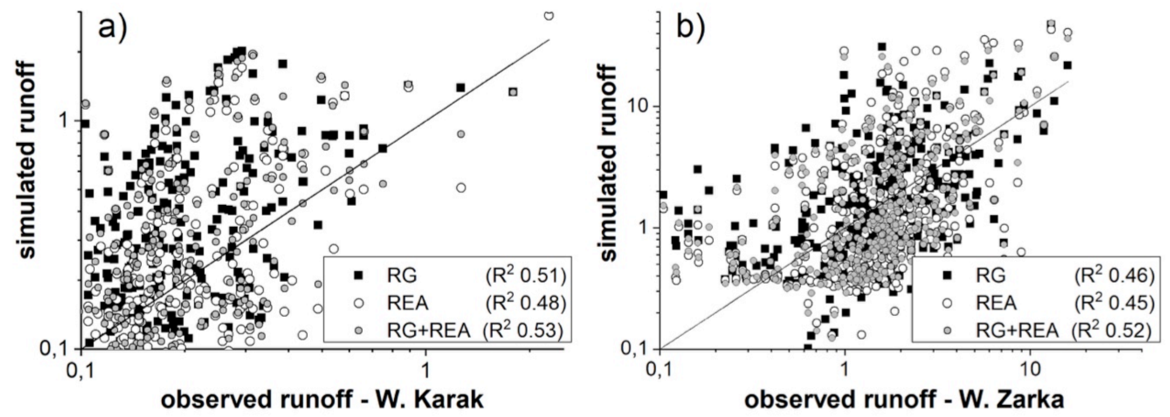

***Fig. 4:** Comparison of observed and simulated runoff at 2 exemplary catchments a) Wadi Karak and b) Wadi Zarka. The results are presented as function of applied input data: (i) available rain gauge (RG) data (black squares), (ii) rainfall reanalysis (REA) data (white circles) and (iii) combination of both RG+REA data (grey circles). The black line indicates the 1:1 line.*

4.3 Calibration and Validation

The standard split-sample tests (see e.g., Klemeš, 1986) were used for the calibration-validation approach. Observed total runoff from catchments draining towards the JDSR (Fig. 2A, Table 2) was used to calibrate the a-priori model and validate the simulated runoff. Since runoff is composed of direct surface runoff (*DQ*) and baseflow (*BQ*), the model was calibrated step-by-step against both (*DQ* and *BQ*), to identify the best parameter sets. That process revealed that baseflow dynamic is predominantly controlled by groundwater reservoirs GWS1 and GWS2. For this reason, only k_1, n_1, k_2 and n_2 were adjusted by best-fit method, while other parameters remained constant (Table 6). From Figure 5 it becomes obvious, the highest correlation between simulated and observed runoff was achieved using parameter set k_1=1.8, n_1=1, k_2=40 and n_2=2 (Fig. 4d). To validate the model the simulated annual groundwater recharge rates is compared to available data from studies investigating surface drainage basins (Amro et al., 1999; Schulz et al., 2013; Rödiger et al., 2014) and groundwater basins (Al Kuisi and El-Naqa, 2013; UN-ESCWA and BGR, 2013; Al-Naber, 2016) all over Jordan (Fig.6). The simulated mean annual groundwater recharge rates fit well (R^2 0.96) to those of the previous studies, indicating the validity of the simulated recharge and hence the reproducibility of the general hydrological behavior of the entire study area.

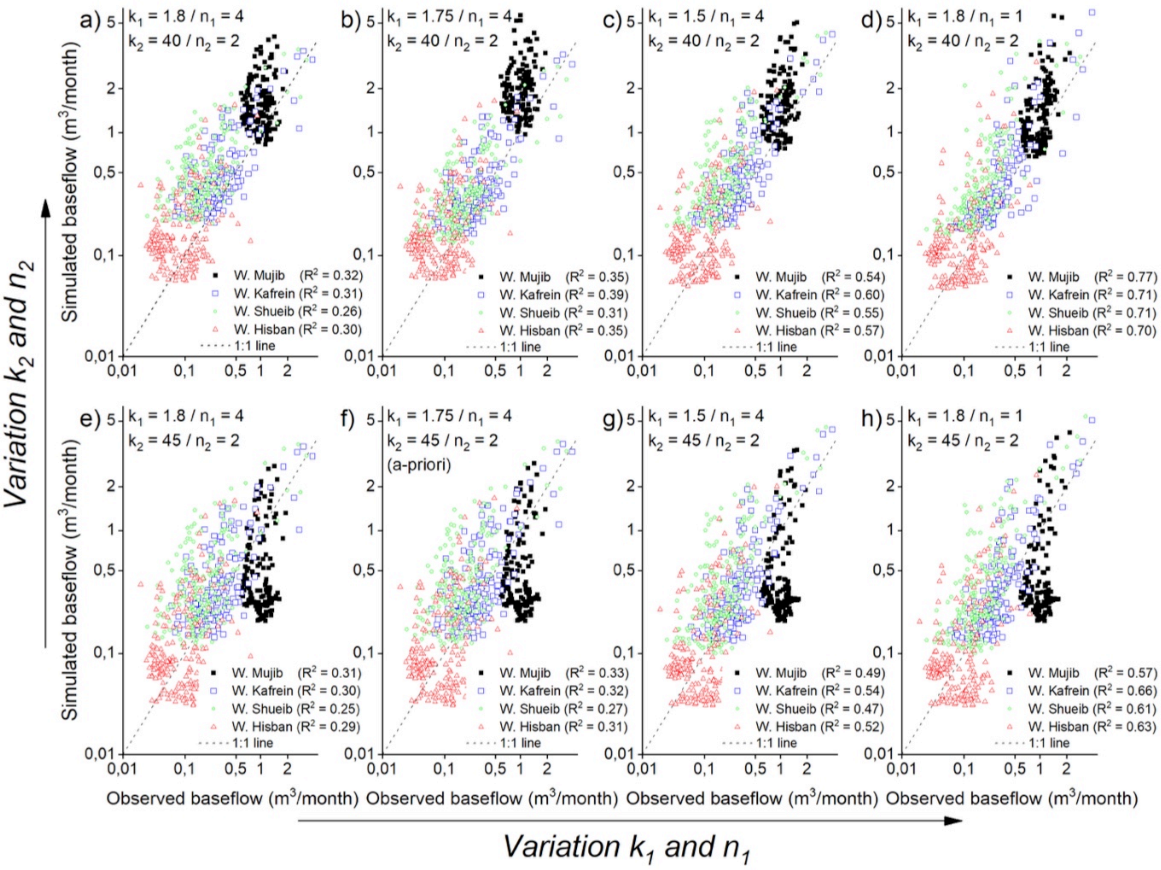

Fig. 5: *Observed vs. simulated baseflow for four exemplary catchments (W. Mujib, W. Kafrein; W. Shueib and W. Hisban) for different parameter sets of k and n, having fast (k_1 and n_1) and slow (k_2 and n_2) reacting reservoirs. The 1:1 line is given as grey line.*

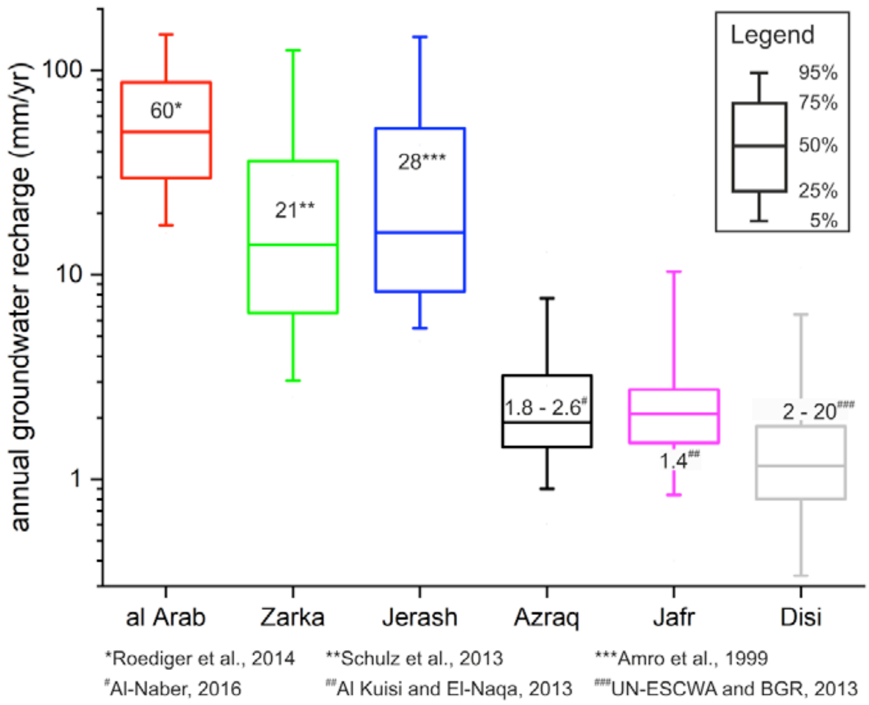

Fig. 6: *Boxplot of calculated groundwater recharge rates for exemplary catchments. For comparison, results from literature sources are shown in or nearby the respective catchment boxes.*

5. Determining Groundwater Depletion

The observed annual GWD in Jordan is most probably not the result of climate change, since climate data show no negative trend in rainfall during the simulation period (1970-2015). Time series of groundwater tables have been assessed for each of the groundwater basins/catchments and any observed annual groundwater depletion (GWD_A) (Fig. 2) is interpreted by Wada et al., (2010) as result of groundwater abstraction, exceeding the natural recharge rates (Equation (2),

$$GWD_A = |GR_A - V_A| \qquad \text{(Eq. 2)}$$

with GR_A [m^3/yr] as groundwater recharge, derived from the hydrological model and aggregated for each groundwater basin, and V_A [m^3/yr] as mean annual groundwater abstraction rates. Hence, in this study we define groundwater depletion (GWD_A) as the rate of groundwater abstraction in excess of natural recharge rate. To determine V_A, the following calculations are necessary.

The changes in groundwater volumes ΔV [m^3] in the basin over the entire observation period T_{obs} in years [a_{obs}] can be determined according to Equation (3) (Hölting and Coldeway, 2013):

$$\Delta V = S \times \Delta h_m \times A_A \qquad \text{(Eq. 3)}$$

with S [-] as storage coefficient (Table 6), Δh_m [m] as mean groundwater table change in the entire basin over the observation period T_{obs} and A_A [m^2] as lateral extension of the aquifer. To reproduce Δh_m for each groundwater level measurement in the respective aquifer, the total groundwater table change Δh_{obs} are calculated according to Equation (4):

$$\Delta h_{obs} = H_t - H_0 \qquad \text{(Eq. 4)}$$

where Δh_{obs} [m] is the total water level change [m], H_0 and H_t represent the absolute groundwater level [m msl.] at the begin and end of the observation period, respectively. Thereafter, all calculated h_{obs} of the respective aquifer in the entire basin are averaged to the mean groundwater table changes h_m. Finally, mean annual groundwater abstraction rate (V_A) [m^3/yr] are estimated according to Equation (5).

$$V_A = \Delta V / T_{obs} \quad \text{(Eq. 5)}$$

with ΔV [m^3] representing change in groundwater storage and T_{obs} as respective length of observation period [a_{obs}] of each of the groundwater basins.

While intensive exploitation of the water resources started in 1975 (Courcier et al., 2005), water levels changes were considered from 1980 onward only to have a consistent time series for the calculation of the mean annual groundwater abstraction rates V_A. To verify the calculations, estimated V_A was compared with available abstraction rates (MWI, 2015). The results are summarized in Table 5.

6. Results and Discussion

The regionalized rainfall pattern represents well the climatic gradients, which show highest rainfall in the NW (>600mm/yr) that steeply declines towards E and SE (Fig. 7a). Being predominantly controlled by precipitation, calculated groundwater recharge rates resemble its spatial pattern with highest rates in the mountainous NW (>200 mm/yr) and rapidly declining rates to less than 20 mm/yr in the JDSR and the eastern and southeastern desert plains (Fig. 7b).

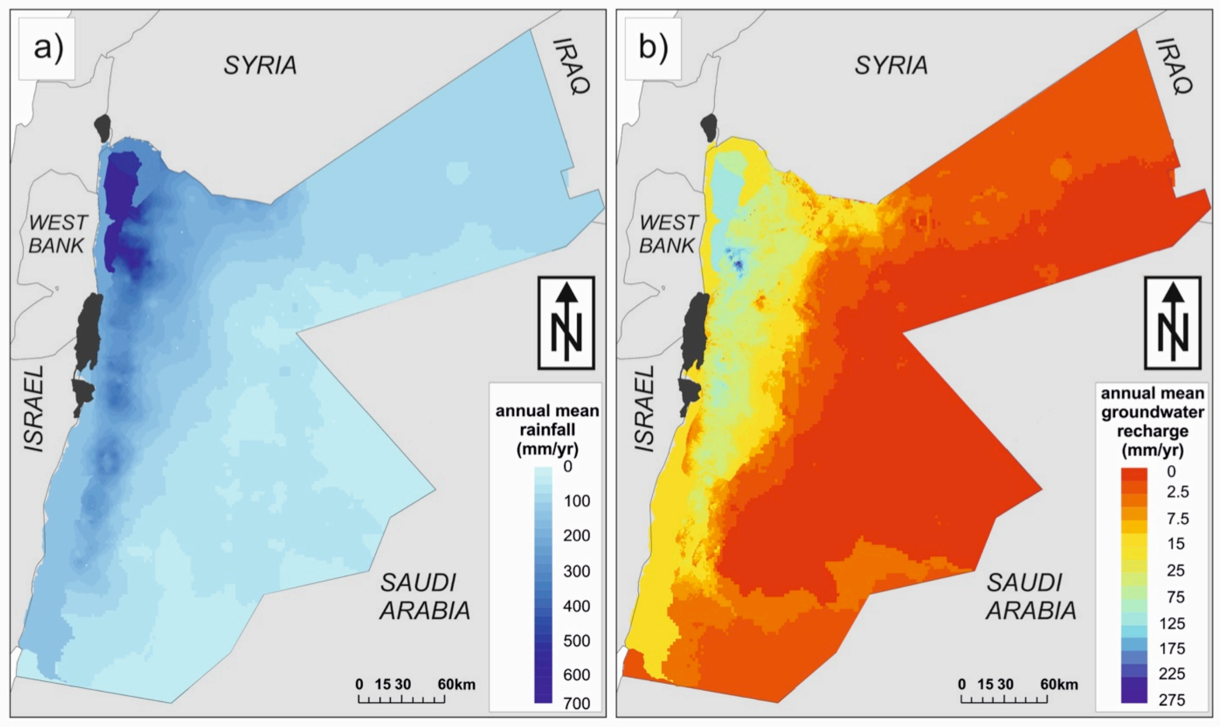

Fig. 7: *(a) Interpolated mean annual rainfall; (b) estimated mean annual groundwater recharge for entire Jordan based on an empirical rainfall–runoff relation in the model period 1970-2015*

Since groundwater recharge depends on precipitation events, it is restricted to the hibernal rainy season (Fig. 8). Average annual precipitation slightly decreases (black dashed line), groundwater recharge (black solid line) remains constant during simulation period but is neglectable (<3mm/yr) during dry years and wherever annual rainfall falls below 50 mm/yr (Fig. 8). From these observations, it can be concluded the nationwide observed aquifer depletion (Figs. 11 and 12) is rather caused by overdraft than climate change.

Applied and evaluated for the entire Kingdom of Jordan, the model gives averaged annual water budget components for the period 1970 to 2015 as follows: rainfall 92.5 mm, actual evapotranspiration 83.9 mm, surface runoff 2.7 mm. The resulting groundwater recharge amounts to 5.9 mm. All resulting values are comparable to data from NWMP (2004).

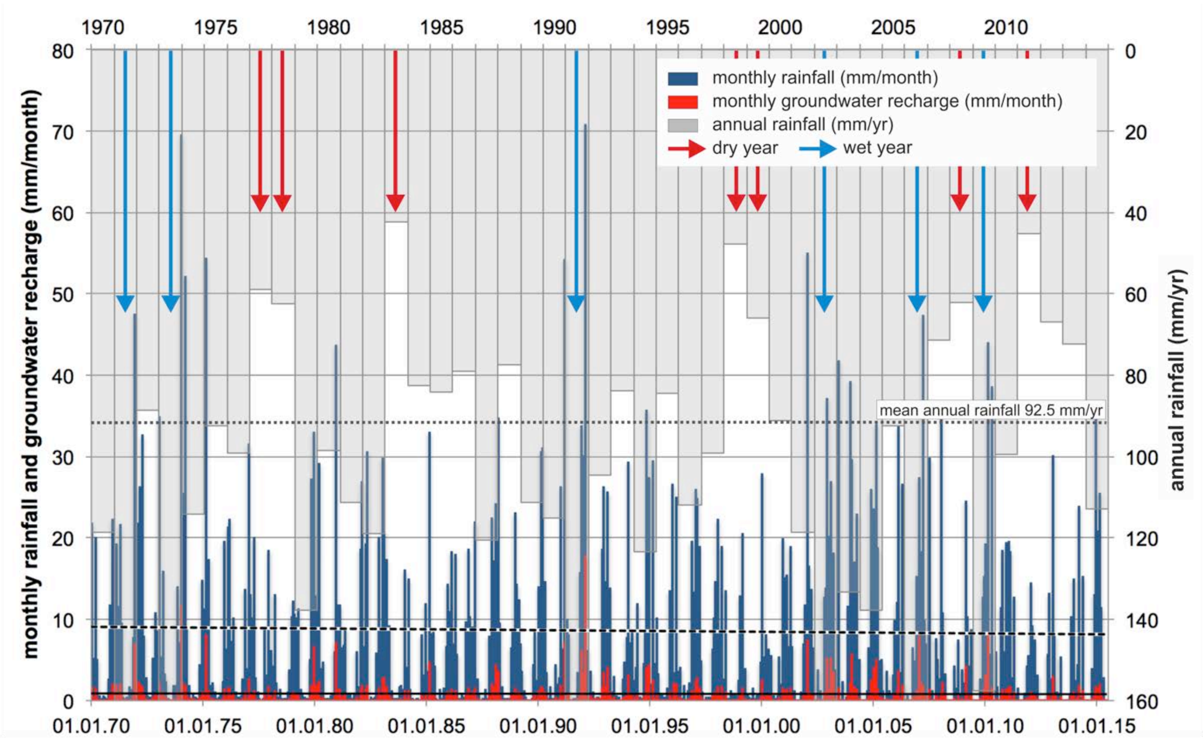

Fig. 8: *Simulated monthly groundwater recharge (red) and monthly rainfall (dark blue) in (mm/month) versus annual rainfall (grey column) in [mm/a]. Trend of monthly rainfall are shown as black dashed line, trend of monthly groundwater recharge is shown as black solid line. Mean annual rainfall is shown as dotted line. Red and blue arrows mark exceptional dry and wet years, respectively, during which average precipitation deviates by >36% from average (Salameh et al., 2018).*

The results by the hydrological model show a general conformity between observed and simulated runoff. Simulated runoff varies within certain ranges which depends on the applied calibration parameter sets (Fig. 9). However, if baseflow sources originate partly from UCA but predominantly from DSA (Figs. 9c-f), simulated runoff is much smaller than observed runoff. That observation reveals the limited applicability of hydrological models in catchments, which either have more than one groundwater stockwork contributing to the baseflow formation or where subsurface drainage basins differ significantly from the surface catchment. In all four catchments (Ibn Hammad, Shueib, Hisban and W. Drea) baseflow is generated from both, UCA and DSA. Models such as J2000g simulate hydrological processes within the catchment of a certain river and consider the water-bearing geological formations as restricted to the same surface catchment boundaries. However, deep large-scale aquifers like the DSA often possess subsurface drainage basins exceeding the overlaying local surface catchments. Hence, in surface catchments, which receive groundwater discharge from both, a local shallow and a much larger deep aquifer, simulated total runoff considerably underestimates baseflow as observed in the Wadis Ibn Hammad and Drea (Figs. 9e, f).

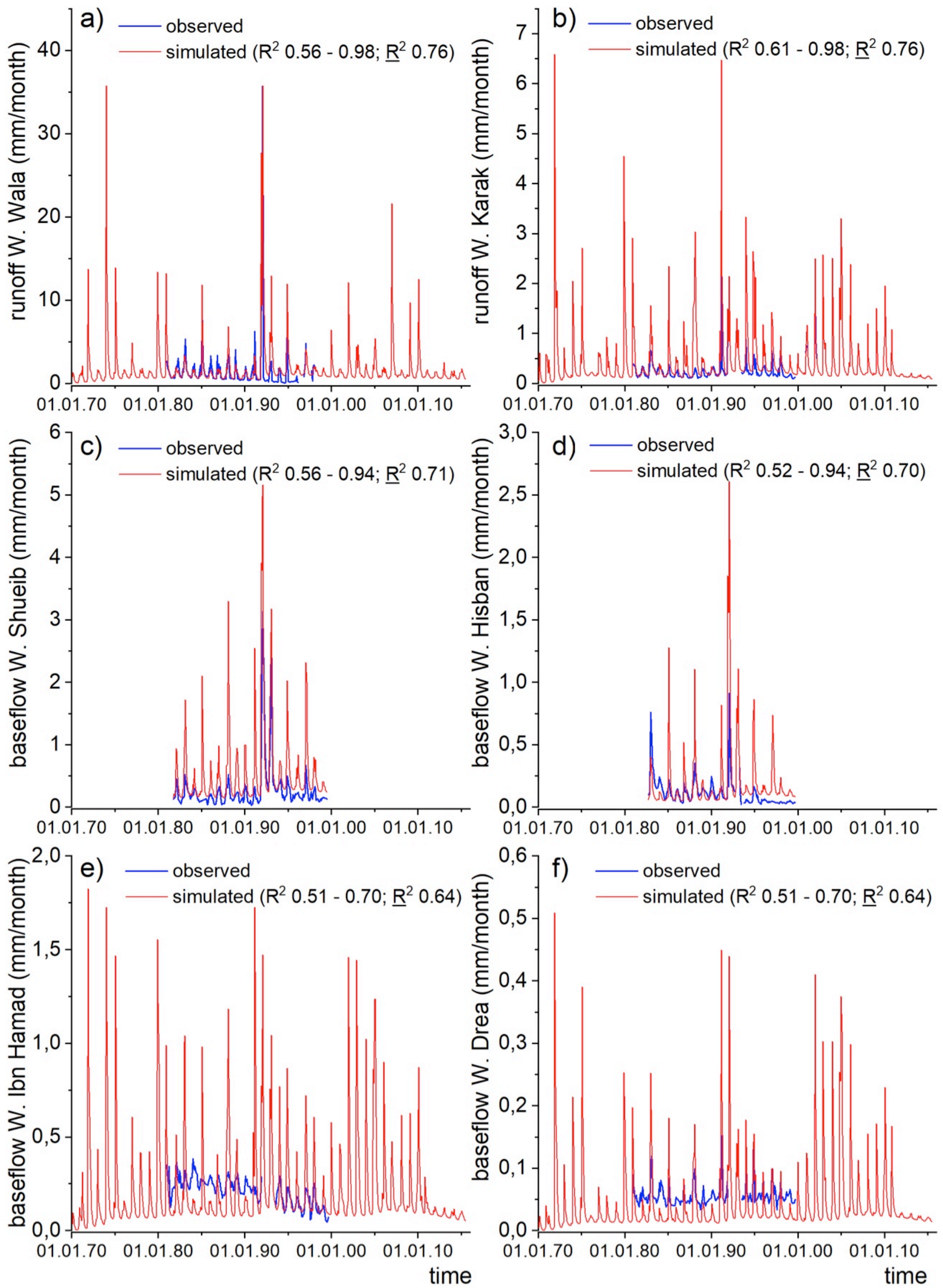

Fig. 9: *Showing exemplary results for simulated vs. observed runoff (a, b) and simulated vs. observed baseflow (c-f), using best fit calibration parameter set k_1=1.8, n_1=1, k_2=40 and n_2=2. Geologically, in catchments a and b the formations of the Upper Cretaceous Aquifer Complex (UCA) dominate and in catchments c-f the Deep Sandstone Aquifer complex (DSA) contributes considerably.*

A second phenomenon is observable in many catchments, where simulated versus observed total monthly runoff may resemble each other (i.e. Wadis Wala, Mujib, Shueib, Isal, Hisban). With onset of the 1990s, simulated runoff significantly exceeds the observed total runoff. A phenomenon, which is even observable in Wadi Ibn Hammad, where J2000g systematically underestimates baseflow due to the above described facts until the 1990s. That discrepancy is interpreted as anthropogenic impact. The increasing overdraft particularly of the UCA, resulted in dropping groundwater tables and accompanied by a reduction of baseflow. Such changing conditions show circumstances, where the applicability of hydrological models is again limited. They are not able to consider groundwater abstraction, which may cause dropping groundwater tables not to mention conditions, where baseflow disappears. Consequently, continuously declining baseflow cannot be processed and the simulated runoff (as sum of baseflow and surface flow) exceeds the observed.

6.1 Future groundwater recharge scenarios

To assess, how groundwater recharge will react on future climate changes, the calibrated hydrological model was forced with climate input files, which base on scenarios of seasonal precipitation changes (RICCAR 2017). The results of both RCP scenarios (4.5 and 8.5) show a dramatically declining average annual groundwater recharge for Mid (2046) and End (2081) of the century (Fig. 10). Depending on the scenario, the decrease of groundwater recharge is low (ca. 1%) taking RCP 4.5, while it worsens to 5-13% until 2046 and 2081, respectively under RCP 8.5 conditions. These results are in good agreement to model-based estimations by Siebert et al. (2014). The most important result is that the Western Mountain Highland, as agricultural backbone of the Kingdom, will suffer most under all scenarios. There, groundwater recharge will be reduced by up to 30 mm/yr. Contrastingly, in the rest of the country, particularly in the eastern and south-eastern desserts, an increase in groundwater recharge of 1-2 mm/yr can be expected.

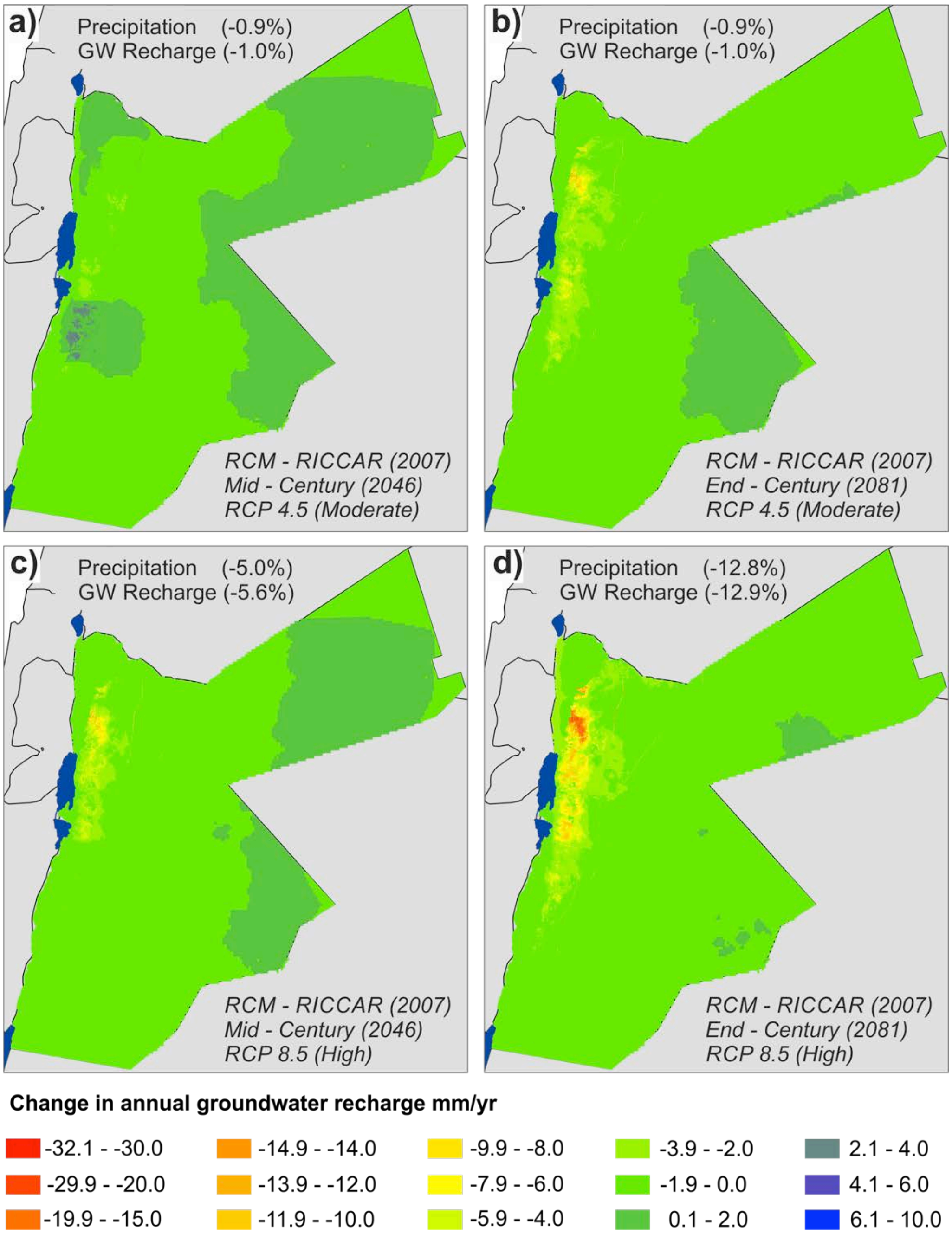

Fig. 10: *Base on predictions of seasonal precipitation changes of RICCAR (2017) the calibrated hydrological model was used to assess changes in groundwater recharge. The shown groundwater recharge difference in mm/a was calculated by average annual groundwater recharge for the scenarios RCP 4.5 (b-c) and RCP 8.5 (e-f), Mid (2046) and End (2081) centuries) minus the average annual groundwater recharge for the time period 1970-2015.*

6.2 Groundwater depletion

Taking the groundwater hydrographs from 123 wells all over Jordan, changes are well observable (Figs. 11, 12). For each basin, a minimum of 5 representative groundwater hydrographs (solid lines in Fig. 11, 12) are used to analyze the average fluctuation range of the water level change (grey areas in Fig. 11, 12). The averaged hydrograph for each basin is shown as dotted line, clearly indicating the generally falling water tables. Courcier et al. (2005) report a moderate drawdown of up to 10 m until mid 1970s for most basins, while the exploitation of the water resources increased sharply during the following decades and caused steep groundwater table droppings until the end of the observation period. The largest drawdown occurred in the heavily exploited A7/B2 aquifer, where groundwater tables dropped locally by more than 40 m (i.e. Fig. 11a). In contrast and due to the late onset of abstraction in the 1990s, groundwater tables in the alluvial aquifers of the JDSR dropped comparably moderate (maximum of 25 m) during the observation period (Fig. 12). The mean groundwater level changes Δh of each groundwater basins are shown in Table 5.

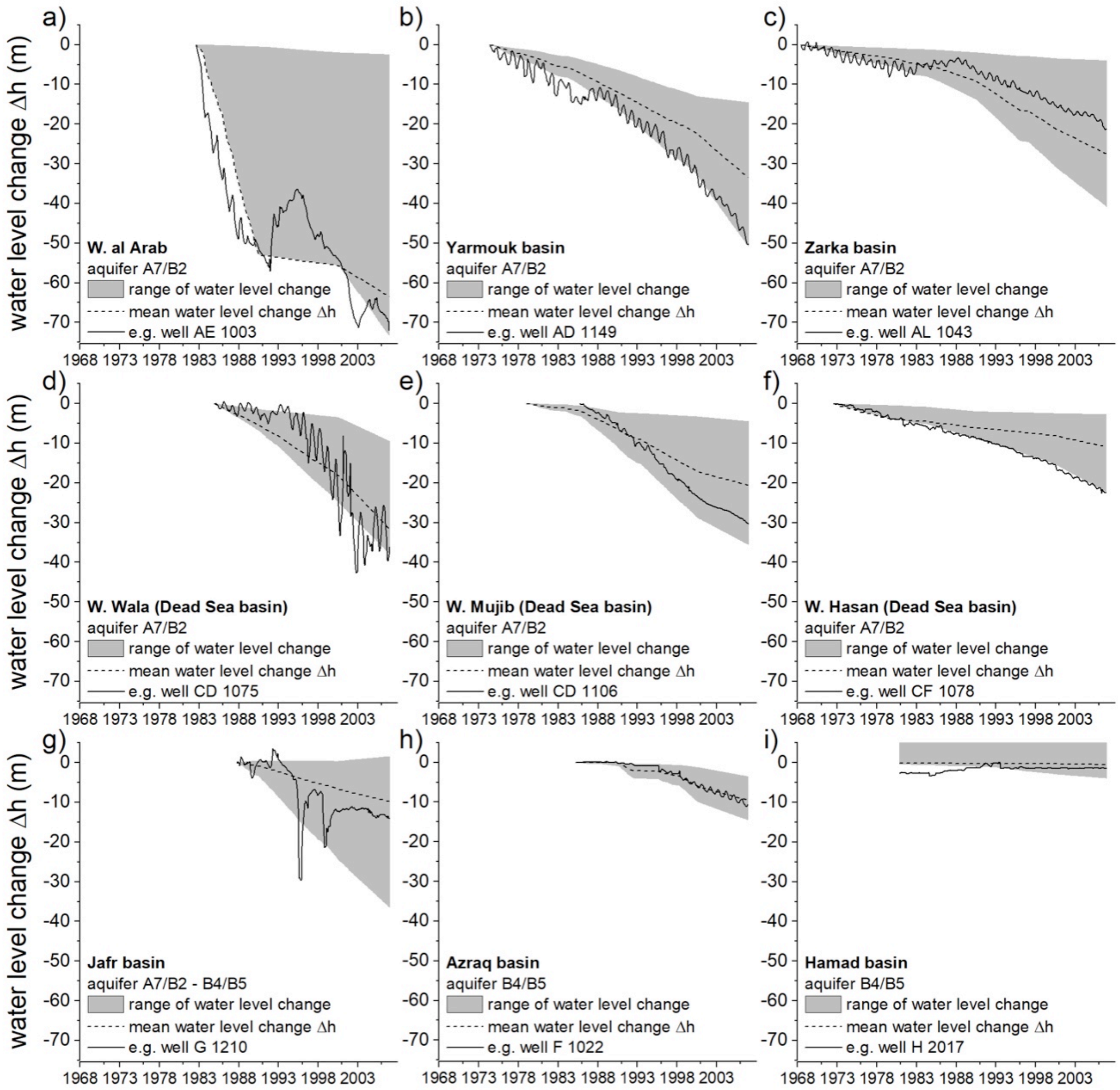

Fig. 11: *Analyses of the groundwater level changes Δh (max, min, mean) for aquifer A7/B2 and B4/B5.*

The mean annual groundwater abstraction rate (V_A) was estimated according to Equation (5). To validate V_A the simulated numbers were set in correlation to abstraction rates provided by UN-ESCWA and BGR (2013) and MWI (2015). Table 5 illustrates, predicted vs. known annual abstraction of the respective groundwater basins are in good agreement. Exceptions are the Yarmouk and Disi basins, which had to be cut at the borders to Syria and Saudi Arabia, respectively, since their extensions into the neighboring countries is unknown. Consequently, the size of the two catchments is too small causing insignificant values for both, groundwater recharge and abstraction rates. The estimated V_A very much varied between the groundwater basins, e.g. in the Ajloun, where almost no abstraction occurs, the abstraction rate was 0.2 MCM/yr only, while in the Zarka catchment the abstraction rate reaches a value of 118.4

MCM/yr. The results show that abstraction rates are up to four times larger than the groundwater recharge in the respective basin. It is apparent, beside A7/B2, that also the shallow B4/B5 and the predominantly fossil and deep DSA (e.g. Jafr and Disi basins) suffer significantly from overdraft.

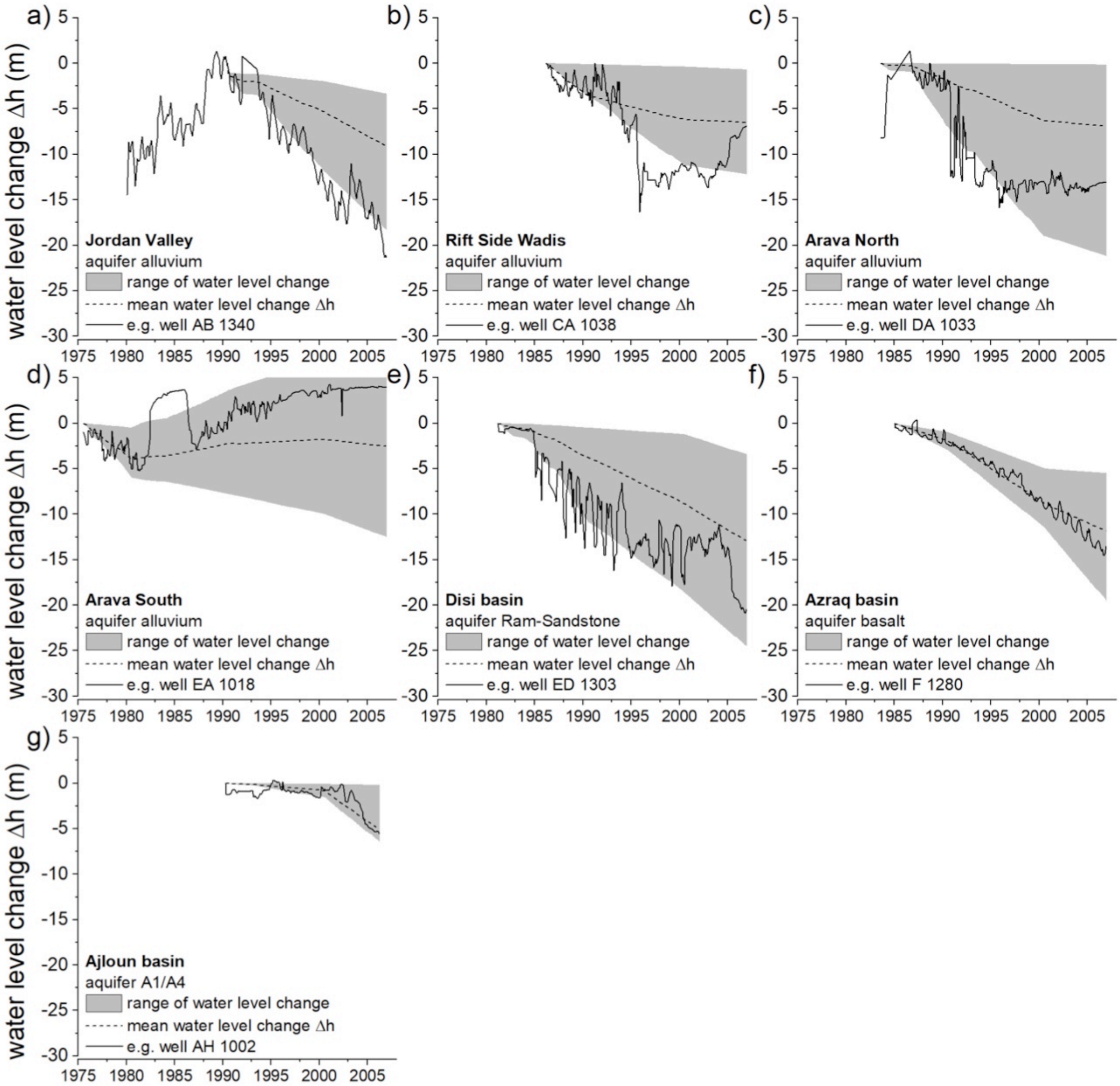

Fig. 12: Analyses of the gw level changes Δh *(max, min, mean) for alluvium aquifer, Ram-Sandstone aquifer, basalt aquifer and aquifer A1/A4.*

All previous results in terms of annual groundwater recharge (Fig. 13a), groundwater level changes (Fig. 13b), annual groundwater abstraction rates (Fig. 13c), and average annual groundwater depletion (Fig. 13d) are mapped for Jordan for the observation period 1970-2015.

Negative values for groundwater depletion (Fig. 13d) indicate basins, where abstraction exceeds the natural recharge. Hot spots of groundwater depletion are observable in Azraq, Disi and Zarqa basins, where deficits exceed 30 MCM/yr (red color). Similar dimensions were estimated analyzing GRACE data (Wada et al., 2010; Döll et al., 2014). According to our analyses, more than three-quarter of Jordan's groundwater resources are seriously affected by strong groundwater depletion. Moreover, the consequences are not only dropping groundwater level and accordingly increased pumping costs, but also the deterioration of water quality that is increasingly observable in each of the affected groundwater basins.

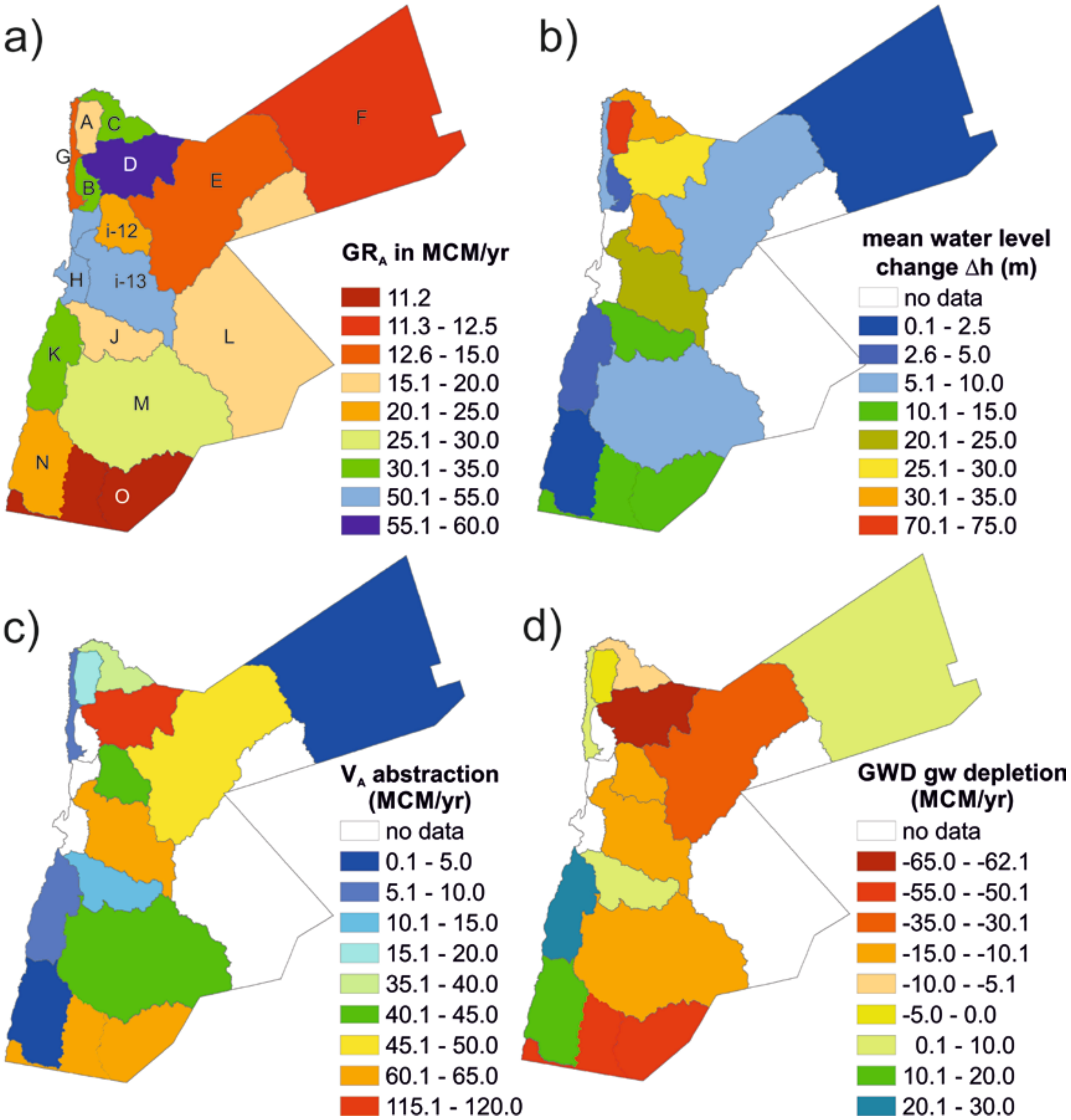

Fig. 13: *(a) Simulated average groundwater recharge by J2000g [MCM/yr] (letters A-O indicate groundwater basins), (b) analyzed mean water level changes Δh [m], c) estimated mean annual*

groundwater abstraction [MCM/yr] and (d) mean annual groundwater depletion [MCM/yr].

Applying the combination of hydrological model and a method to evaluate changing groundwater volumes, a climate-driven systematic decline of groundwater recharge was eliminated as responsible process, while overdraft leads to dropping groundwater tables in Jordan. The major findings are, the intensity of groundwater abstraction from a basin becomes visible through the fact that simulated baseflow by the hydrological model exceeds by far the observed.

7. Conclusions

The aim of the study was to provide an overview about the level of anthropogenic groundwater depletion in Jordan. The very limited data availability that often characterizes arid regions adds a significant challenge in obtaining reliable results. Here, the development of a hydrological model, the interpretations of water level changes and the estimations of annual abstraction rates were realized to evaluate groundwater depletion. The different processing steps were affected by (i) a limited hydrogeological dataset (e.g. hydraulic parameters, water levels) and (ii) incomplete datasets of abstraction rates, precipitation data and hydrograph gauging stations.

The high spatial data uncertainty of rain data in the hydrological model was partly improved by a combination of measured rain gauge data and REA data. It was shown that the proposed approach could help to improve the model adaptations and thus the model prediction. At the example of Jordan the limits of hydrological modeling when predicting heavily overused groundwater resources could be clearly shown. The falling groundwater levels in the study area lead to dropping baseflow and hence observable surface runoff. That process cannot be represented in the hydrological model, which means that a continuously decreasing baseflow cannot be processed and the simulated runoff (as the sum of baseflow and surface runoff) exceeds the observed value.

Nevertheless, the modeling enables the seasonal fluctuations in groundwater recharge to be reconstructed over a period of 45 years. Results show a very slight decrease in the rainfall, which does not affect groundwater recharge.

We found that changes in groundwater recharge were mainly driven by changes of precipitation. Base on predictions of seasonal precipitation changes of RICCAR (2017) we estimated the potential changes of groundwater recharge: following RCP 4.5 groundwater recharge ranges between -1% and +7%. In contrast, a general decline in groundwater recharge between -5 and -13% is expected under RCP 8.5. Furthermore, all scenarios show that the major changes of groundwater recharge are highly likely in the Jordan Mountains with decreases of over 30mm/yr and increases of over 10mm/yr. The RCP 4.5 and 8.5 scenarios also show that an increase in groundwater recharge of 1-2 mm/yr can be expected in the Eastern Desert.

The estimated abstraction rates indicate that beyond the overexploited aquifer A7/B2, also the B4/B5 aquifers and the predominant fossil groundwater reservoirs in the southern part of Jordan are highly affected by overdraft.

The intense abstraction and the comparable low amounts of natural groundwater recharge are reflected by the dimension of groundwater depletion. In some parts of the country the depletion reaches more than 30 MCM/yr, particularly in the Zarka and Azraq basins that both host the City of Amman and its periphery. Apart from those, also in the predominant fossil groundwater reservoirs in southern part of the country we observe higher depletion values. Based on the proposed methods we were able to show that already three-quarters of the country are affected by severe groundwater depletion.

We consider the applied methodology as relevant and transferable to other data- and water scarce areas worldwide, allowing (i) a relative quick estimation of groundwater reservoir development on a national scale and (ii) investigation of long-term effects of overdraft.

Acknowledgments

The authors are grateful to the Helmholtz Association of German Research Centers, for funding the DESERVE-project (VH-VI-527). The authors particularly thank the Ministry of

Water and Irrigation Jordan and the Water Authority of Jordan for fruitful cooperation and the kind provision of data. We thank Professor Harald Kunstmann and Gerhard Smiatek from KIT for providing the rainfall reanalysis data.

References:

Abdulla, F.A., Al-Khatib, M.A. and Al-Ghazzawi, Z.D., 2000. Development of groundwater modeling for the Azraq Basin, Jordan. Environmental Geology. 40, 11-18. https://doi.org/10.1007/s002549900105.

Abdulla, F. and Al-Assa'd, T., 2006. Modeling of groundwater flow for Mujib aquifer, Jordan. J. Earth Syst. Sci. 115, 289-297. https://doi.org/10.1007/BF02702043.

Al Kuisi, M. and El-Naqa, A., 2013. GIS based Spatial Groundwater Recharge estimation in the Jafr basin, Jordan – Application of WetSpass models for arid regions. Revista Mexicana de Ciencias Geológicas. 30, 96-109.

Al-Naber, M., 2016. Jordan – Azraq basin case study. IWMI Report 12, Groundwater governance in the Arab World. US AID.

Allen, R.G., Pereira, L.S., Raes, D., Smith, M., 1998. Crop evapotranspiration - Guidelines for computing crop water requirements. FAO Irrig. and Drain. Paper 56, Food and Agric. Orgn. of the United Nations, Rome.

Alley, W.M., Reilly, T.E., and Franke, O.L., 1999. Sustainability of ground-water resources: U.S. Geological Survey Circular. 1186, 79. https://doi.org/10.3133/cir1186.

Al-Omari, A., Al-Quraan, S., Al-Salihi, A., Abdulla, F., 2009. A water management support system for Amman Zarqa Basin in Jordan. Water Resour Manage. 23, 3165–3189. https://doi.org/10.1007/s11269-009- 9428-z.

Amro, H., Kilani, S., Jawawdeh, J., Abd El- Di, I. and Rayan, M., 1999. Isotope based assessment of groundwater recharge and pollution in water scarce areas: A case study in Jordan. (IAEA-TECDOC--1246). International Atomic Energy Agency (IAEA).

Ayed, R. 1996. Hydrological and hydrogeological study of the Azraq basin. PhD Thesis. Univ

Baghdad, Baghdad, Iraq,pp 85 –96.

Berndtsson, R., Larson, M., 1987. Spatial variability of infiltration in a semi-arid environment. J. Hydrol. 90, 117–133. https://doi.org/10.1016/0022-1694(87)90175-2.

Changnon, S. A., Huff, F. A., & Hsu, C. F. 1988 Relations between precipitation and shallow groundwater in Illinois. Journal of Climate. 1,1239–1250. https://doi.org/10.1175/1520-0442(1988).

Courcier, R., Venot, J.P. and Molle, F., 2005. Historical transformations of the lower Jordan river basin (in Jordan): Changes in water use and projections (1950-2025). Comprehensive Assessment Research Report 9. Colombo, Sri Lanka: Comprehensive Assessment Secretariat.

De Vries, J. J., & Simmers, I. 2002. Groundwater recharge: An overview of processes and challenges. Hydrogeology Journal. 10, 5–17. https://doi.org/10.1007/s10040-001-0171-7.

Dillon, P., Escalante, E.F. and Tuinhof, A., 2012. Management of aquifer recharge and discharge processes and aquifer storage equilibrium. Groundwater Governance Thematic Paper 4, Rome, GEF-FA.

Döll, P., Schmied, H.M., Schuh, C., Portmann, F.T. and Eicker, A., 2014. Global-scale assessment of groundwater depletion and related groundwater abstractions: Combining hydrological modeling with information from well observations and GRACE satellites. Water Res. Res. 50, 5698–5720. https://doi.org/10.1002/2014WR015595.

El-Naqa, A. 1993. Hydrological and hydrogeological characteristics of Wadi el Mujib catchment area, Jordan. Environmental Geology. 22, Issue 3. https://doi.org/10.1007/BF00767411.

Dorman, J.L., Sellers, P.J., 1989. A global climatology of albedo, roughness length and stomata] resistance for atmospheric general circulation models as represented by the Simple Biosphere Model. J. Appl. Meteorol. 28, 833–855. https://doi.org/10.1175/1520-0450(1989)028<0833:AGCOAR>2.0.CO;2.

FAO 2015. Regional Overview of Food Insecurity – Near East and North Africa: Strengthening Regional Collaboration to Build Resilience for Food Security and Nutrition, Cairo, Egypt, FAO.

Flügel, W.A., 1993. Hierarchically structured hydrological process studies to regionalize interflow in a loess covered catchment near Heidelberg, IAHS Publ. 212, 215-223.

Gleeson, T., VanderSteen, J., Sophocleous, M. A., Taniguchi, M., Alley, W. M., Allen, D. M. and Zhou, Y., 2010. Commentary: Groundwater sustainability strategies, Nat. Geosci. 3, 378–379. https://doi.org/10.1038/ngeo881.

Goode, D.J., Senior, L.A., Subah, Al. and Jaber, A., 2013. Groundwater-Level Trends and Forecasts, and Salinity Trends, in the Azraq, Dead Sea, Hammad, Jordan Side Valleys, Yarmouk, and Zarqa Groundwater Basins, Jordan; Open-File Report 2013-1061; U.S. Department of the Interior: Washington, DC, USA; U.S. Geological Survey: Reston, VA, USA.

Hanasaki, N., Kanae, S., Oki, T., Masuda, K., Motoya, K., Shirakawa, N., Shen, Y. and Tanaka, K., 2008. An integrated model for the assessment of global water resources – Part 2: Applications and assessments, Hydrol. Earth Syst. Sci. 12, 1027–1037. https://doi.org/10.5194/hess-12-1027-2008.

Hölting, B. and Coldewey, W.G., 2008. Hydrogeologie: Einführung in die Allgemeine und Angewandte Hydrogeologie. Spektrum Akademischer Verlag.

Houria, B., Mahdi, K., Zohra, T.F., 2020. Hydrochemical Characterisation of Groundwater Quality: Merdja Plain (Tebessa Town, Algeria). Civil Engineering Journal. 6, 2. https://doi.org/10.28991/cej-2020-03091473.

IPCC, 2014. Climate Change 2014: Synthesis Report. Contribution of Working Groups I, II and III to the Fifth Assessment Report of the Intergovernmental Panel on Climate Change [Core Writing Team, R.K. Pachauri and L.A. Meyer (eds.)]. IPCC, Geneva, Switzerland, 151 pp.

Klemes, V., 1986. Operational testing of hydrological simulation models. Hydrological Sciences Journal. 31(1), 13-24. https://doi.org/10.1080/02626668609491024

Körner, Ch., 1994. Leaf diffusive conductances in the major vegetation types of the globe. In: Schulze, E.D., Goldwell, M.M. (Eds.), Ecophysiology of Photosynthesis, Ecological Studies, Springer, Berlin.

Kralisch, S., Krause, P., 2006. JAMS – A Framework for Natural Resource Model Development and Application. In: Gourbesville, P., Cunge, J., Guinot, V., Liong, S.-Y. (Eds.), Proceedings of the 7th International Conference on Hydroinformatics.

Krause, P., 2001. Das hydrologische Modellsystem J2000: Beschreibung und Anwendung in großen Flußeinzugsgebieten. Schriften des Forschungszentrums Jülich: Reihe Umwelt/Environment; Band 29.

Krause, P., Hanisch, S., 2009. Simulation and analysis of the impact of projected climate change on the spatially distributed waterbalance in Thuringia, Germany. Adv. Geosci. 21, 33–48. https://doi.org/ 10.5194/adgeo-21-33-2009.

Krause, P., Biskop, S., Helmschrot, J., Flügel, W.-A., Kang, S., Gao, T., 2010. Hydrological system analysis and modelling of the Nam Co Basin in Tibet. Adv. Geosci. 27, 29–36. https://doi.org/10.5194/adgeo-27-29-2010.

Kunstmann, H., Suppan, P., Heckl, A. and Rimmer, A., 2007. Regional climate change in the Middle East and impact on hydrology in the Upper Jordan catchment. Quantification and Reduction of Predictive Uncertainty for Sustainable Water Resources Management (Proceedings of Symposium HS2004 at IUGG2007, Perugia, July 2007). IAHS Publ. 313, 2007.

Litovsky, A., Wennubst, A.P. and Joubert, P., 2016. CEO briefing: Global depletion of aquifers. Earth Security Group.

MacDonald, A., Bonsor, H., Ahmed, K., Burgess; W.G., Basharat, M., Calow, R.C., Tucker, J., Dixit, A., Yadav, S.K., Foster, S.S.D., Gopal, K., Rao, M.S., Lapworth, D.J., Lark, R.M., Moench, M., Mukherjee, A., Shamsudduha, M., Smith, L., Taylor, R.G., van Steenbergen, F., 2016. Groundwater quality and depletion in the Indo-Gangetic Basin mapped from in situ observations. Nature Geosci. 9, 762–766. https://doi.org/10.1038/ngeo2791.

Ministry of Agriculture, Jordan, 1994. National Soil Map and Land Use Project – The Soils of Jordan, Level 2: Semi-detailed Studies, vol. 2. Main Report, Ministry of Agriculture, Jordan.

MWI (2015): Open files from Water Information System, hosted at Ministry of Water and Irrigation of the Kingdom of Jordan (MWI).

Nash, J.E., 1958. The form of the instantaneous unit hydrograph. Int. Assoc. Sci. Hydrol., Publ. n62, 3.

NWMP – National Water Master Plan 2004. – The Hashemite Kingdom of Jordan, Ministry of Water and Irrigation (MWI).

Purushotham, D., Prakash, M.R. & Narsing Rao, A., 2011. Groundwater depletion and quality deterioration due to environmental impacts in Maheshwaram watershed of R.R. district, AP (India). Environ Earth Sci. 62, 1707–1721. https://doi.org/10.1007/s12665-010-0666-4.

Richey, A. S., Thomas, B. F., Lo, M.-H., Reager, J. T., Famiglietti, J. S., Voss, K., Swenson, S. and Rodell M., 2015. Quantifying renewable groundwater stress with GRACE, Water Resour. Res. 51. https://doi.org/10.1002/2015WR017349.

RICCAR 2020. Regional Initiative for the assessment of Climate Change impacts on water resources and socio-economic vulnerability in the Arab Region. http://www.escwa.un.org/RICCAR (accessed 11 February 2020).

Rimawi, O., El-Naqa, A., Al Zubi, Y., Jiries, A. and Abu-Hamatteh, Z.S., 2012. Groundwater modeling of Eshidya phosphate mining area , southern Jordan. International Water Technology Journal. 2.

Rödiger, T., Geyer, S., Mallast, U., Merz, R., Krause, P., Fischer, C., & Siebert, C., 2014. Multi-response calibration of a conceptual hydrological model in the semiarid catchment of Wadi al Arab, Jordan. Journal of Hydrology. 509, 193–206. https://doi.org/10.1016/j.hydrol.2013.11.026.

Rödiger, T., Magri, F., Geyer, S., Morandage, S.T., Subah, A., Alraggad, M. and Siebert, Ch., 2017. Assessing anthropogenic impacts on limited water resources under semi-arid conditions: three-dimensional transient regional modelling in Jordan. Hydrogeol J. 25, 2139. https://doi.org/10.1007/s10040-017-1601-5.

Sachse, A., Fischer, C., Laronne, J.B., Hennig, H., Marei, A. Kolditz, O. and Rödiger, T., 2017. Water balance estimation under the challenge of data scarcity in a hyperarid to Mediterranean region. Hydrological Processes. 31, 13. https://doi.org/10.1002/hyp.11189.

Salameh, E., Shteiwi, M., and Al Raggad, M., 2018. Water Resources of Jordan. Springer

Scheffran, J., and Brauch, H. G., 2014. Conflicts and security risks of climate change in the Mediterranean region, in: Goffredo, S. & Dubinsky, Z. (eds.), The Mediterranean Sea: Its history and present challenges, Berlin, pp. 625-640, Springer.

Schulz, S., Siebert, C., Rödiger, T., Al-Raggad, M., & Merz, R., 2013. Application of the water balance model J2000 to estimate groundwater recharge in a semi-arid environment—A case study in the Zarqa River catchment, NW-Jordan. Environmental Earth Sciences. 69(2), 605–615. https://doi.org/10.1007/s12665-013-2342-y.

Schulze, E.D., Kelliher, F.M., Körner, C., Lloyd, J., Leuning, R., 1994. Relationship between maximum stomatal conductance, ecosystem surface conductance, carbon assimilation rate and plant nitrogen nutrition: a global ecology scaling exercise. Ann. Rev. Ecol. Syst. 25, 629–660.

Shawaqfah, M., Alqdah, I. and Adaileh, A., 2016. Development of three-dimension groundwater model for Al-Corridor Well Field, Amman-Zarqa Basin. Int. Journal of Environm. and Ecological Engineering..3.

Siebert, C., Rödiger, T., Mallast, U., Gräbe, A., Guttman, J., Laronne, J.B., Storz-Peretz, Y., Greenman, A., Salameh, E., Al-Raggad, M., Vachtman, D., Zvi, A.B., Ionescu, D., Brenner, A., Merz, R., Geyer, S., 2014. Challenges to estimate surface- and groundwater flow in arid regions: The Dead Sea catchment. Sci. Total Environ. 485-486, 828 – 841. https://doi.org/10.1016/j.scitotenv.2014.04.010.

Smiatek G., Heckl, A. and Kunstmann, H., 2014: High resolution climate change impact analysis on expected future water availability in the Upper Jordan Catchment/Near East. Journal of Hydrometeorology. 15 (4). https://doi.org/10.1175/JHM-D-13-0153.1.

Tilch, N., Uhlenbrook, S., & Leibundgut, C. 2002. Regionalisierungsverfahren zur Ausweisung von hydrotopen in von periglazialem Hangschutt geprägten Gebieten. Grundwasser, 7(4), 206–216. https://doi.org/10.1007/s007670200032.

UNCCD 2012. http://www.unccd.int/en/programmes/Thematic-Priorities/water/Pages/default.aspx (accessed 11 October 2017).

UN-ESCWA and BGR (United Nations Economic and Social Commission for Western Asia;

Bundesanstalt für Geowissenschaften und Rohstoffe). 2013. Inventory of Shared Water Resources in Western Asia. Beirut, https://waterinventory.org/sites/waterinventory.org/files/00-Information-brochure-Water-Inventory-web.pdf (accessed 28 October 2017).

USGS 2016. https://earthexplorer.usgs.gov (accessed 15 January 2018).

Wada, Y., van Beek, L.P.H., van Kempen, C.M., Reckman, J.W.T.M., Vasak, S. and Bierkens, M.F.P., 2010. Global depletion of groundwater resources. Geophysical Research Letter. 37. https://doi.org/10.1029/2010GL044571.

World Bank 2020. https://data.worldbank.org/country/jordan (accessed 30 March 2020).

Zektser, I. S. and Loaiciga, H. J., 1993. Groundwater fluxes in the global hydrologic cycle past, present, and future. Journal of Hydrology. 144, 405–427. https://doi.org/10.1016/0022-1694(93)90182-9.